A Nonlinear Structural Concept for Drag-Reducing Compliant Walls

Edward L. Reiss*
Northwestern University, Evanston, Illinois

A mechanism of drag reduction for turbulent flows over flat plates is investigated. It employs Bushnell's hypothesis that compliant walls produce drag reduction by interfering with the formulation and bursting of the near-wall, low-speed streaks in a turbulent boundary layer. It is shown that the required amplitudes and frequencies of the wall motion might be achieved by using slightly curved elastic walls and the resulting large-amplitude motions of snap buckling of the walls. A simple structural model of an arch is used in the analysis. From the solution of the arch problem it is shown that the required structural motions can be obtained for compliant walls constructed from materials such as Mylar.

I. Introduction

NEARLY one-half of the total drag of high-subsonic-speed, long-range aircraft is a result of viscous drag caused by turbulent skin friction. Thus, any method that substantially reduces this drag will dramatically affect future aircraft design and the general question of energy conservation.

In a series of pioneering experiments, Kramer (see, e.g., Refs. 1 and 2) demonstrated that significant drag reduction can be achieved in the motion of bodies under water by coating their surfaces with compliant materials. Kramer's most successful experiments occurred for compliant materials that attempted to simulate dolphin skins. The precise mechanism for the reduction of drag by compliant surfaces is now known. Kramer and other investigators conjectured that the drag reduction resulted from a delay in the transition from laminar to turbulent flow; but it is presently believed[3] that this effect is unimportant at the large Reynolds numbers in Kramer's experiments. However, experimental results on drag reduction by compliant walls for airflows are inconclusive; see Ref. 3 for a critical and detailed survey.

In the past decade, fundamental experimental advances have been made in understanding how turbulence is produced in a turbulent boundary layer. These experiments show that there is an organized sequence of flow events that give rise to boundary-layer turbulence. The basic feature of such turbulence-producing flows is the formation and subsequent motion of fluid "bursts" near the wall. The experiments suggest that most of the turbulence, and hence most of the drag, is produced during the bursts and their motion away from the wall. A discussion and summary of the burst formation process is given in Ref. 3.

Bushnell et al.[3,4] have conjectured that compliant walls produce drag reduction by interfering and altering the bursting process. This compliant wall burst modulation theory requires the walls to respond with sufficiently large amplitude and high frequency. A variety of compliant walls have been employed using different materials and different structural configurations. They are described in Refs. 3-5. However, none of these walls have provided the required motions or resulted in significant drag reductions for airflows.

In this paper, we present a new structural mechanism that may produce the desired wall motion. The method employs slightly curved walls subjected to fluid pressures, and the ensuing nonlinear large-amplitude motion of the wall. That is, it relies on the dynamics of the snap buckling of the curved elastic plates. A simplified model of the flow over a curved plate is analyzed to demonstrate that the geometrical and physical parameters of the plate can be selected so that it responds with the required amplitudes and frequencies. The model consists of a shallow elastic arch (which is equivalent to a wide cylindrical plate) that is subjected to a static pressure difference $P(X)$ applied across its surface, as shown in Fig. 1. This pressure roughly simulates the combined effects of the mean aerodynamic forces on the top surface of the arch and an external pressure applied to the bottom surface of the arch. It is assumed that this applied pressure can be varied independent of the flow. Thus, the interaction of the arch on the airflow is neglected in the model. A further simplification is made by assuming that the undeformed shape of the arch, the pressure, the initial disturbances, and the response vary sinusoidally in X. Then it is possible to solve the resulting mathematical model exactly.

The static equilibrium states of the arch are analyzed in Sec. III. As the pressure increases from zero, the arch assumes stable equilibrium states with relatively small amplitudes. They are called unbuckled states. At a critical value of the pressure, the unbuckled state becomes unstable because there are no nearby equilibrium states for pressures slightly greater than the critical value. Then due to any small disturbance the shell jumps, or snap buckles, resulting in a large-amplitude periodic motion. This motion is obtained in Sec. IV in terms of the geometrical and material parameters of the arch and the amplitudes of the fluid-imposed disturbances.

In Sec. V these results are employed to show that, for experimentally feasible arch geometries and for certain materials such as Mylar, the amplitudes and frequencies of the motion are within the limits required by Bushnell's hypothesis for drag-reducing compliant walls. However, the present theory is not yet complete because it was assumed in the analysis that the fluid and arch motions are decoupled. A more refined theory is required that accounts for this fluid/solid interaction.

II. Formulation of the Dynamic Snapping of an Elastic Arch

A shallow elastic arch of length L, cross-sectional area a, and cross-sectional moment of inertia I is subjected to a lateral force per unit length $P(X,T)$ shown by the arrows in Fig. 1. Here X is the axial coordinate of the arch, $0 \le X \le L$, and T is the time. The arch is assumed to be simply supported

Received Oct. 15, 1982; revision received May 19, 1983.

*Professor of Applied Mathematics, Department of Engineering Sciences and Applied Mathematics.

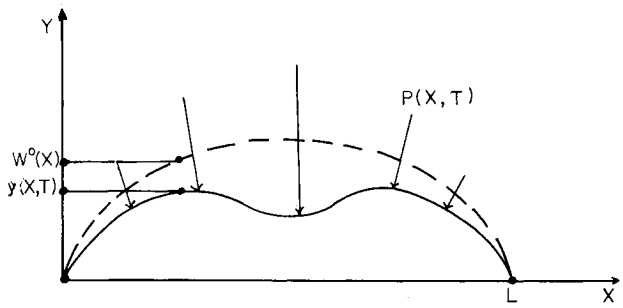

Fig. 1 Geometry of the elastic arch.

at the ends $X=0,L$. The vertical position of the undeformed arch is $Y=W^{\circ}(X)$, where W° is a specified function. It is indicated by the dashed curve in Fig. 1. If the deformed position of the arch is denoted by $Y=y(X,T)$ and is indicated by the solid curve in Fig. 1, then the "excess" vertical displacement $W(X,T)$ is defined by

$$W(X,T) \equiv W^{\circ}(X) - y(X,T) \tag{1}$$

The pressure P is a specified function because the action of the arch on the airflow is neglected. In the combined fluid/solid problem, P will depend upon W and its derivatives through the aerodynamic forces acting on the surface of the arch.

It can be shown[6-8] that the equations of motion of the arch can be reduced to an initial-boundary value problem for an integro-partial differential equation† for W. The solution of this problem depends on the structural parameter ℓ which is defined by

$$\ell \equiv L^2 a/I \tag{2}$$

For sinusoidal arches with sinusoidal initial conditions and static but sinusoidal pressures, that is,

$$W^{\circ} = H\Phi(X), \qquad P(X,T) = Q\Phi(X)$$
$$W(X,0) = F\Phi(X), \qquad W_T(X,0) = 0 \tag{3}$$

where $\Phi \equiv \sin \pi X/L$ and the constants H, Q, and F are the maximum values of the respective quantities in Eq. (3), the problem has the solutions[6]

$$W(X,T) = LA(t)\Phi(X) \tag{4}$$

Here t is a dimensionless time that is defined by

$$t \equiv (\pi^2/2L)(E/\rho)^{1/2} T \tag{5}$$

and $A(t)$ satisfies the initial value problem,

$$A'' + \alpha A - 3hA^2 + A^3 - q = 0$$
$$A(0) = F/L, \qquad A'(0) = 0 \tag{6}$$

A prime denotes differentiation with respect to t and the parameters h, α, and q are defined by

$$h \equiv H/L, \qquad \alpha \equiv 2(h^2 + 2\ell), \qquad q \equiv (4/\pi^4)(L/Ea)Q \tag{7}$$

†With a suitable definition of the parameter (EI/a), this problem describes the motion of a cylindrical panel that is curved in the direction of the flow and is infinitely long transverse to the flow.

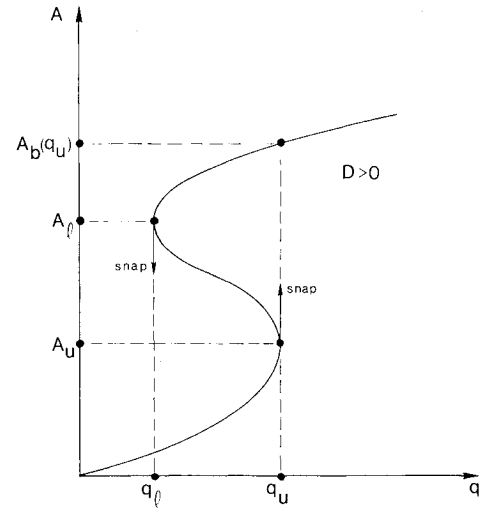

Fig. 2 Response diagram for the static states of the elastic arch.

III. The Static States

It follows from Eq. (6) that the amplitudes of the equilibrium positions of the arch satisfy the cubic equation,

$$q = \alpha A - 3hA^2 + A^3 \tag{8}$$

The number of real roots in Eq. (8) depends on the sign of the discriminant,

$$D \equiv h^2 - \alpha/3 = (h^2 - 4\ell)/3 \tag{9}$$

We consider only arches with $D>0$. Then there is a unique static state for q in the intervals, $q<q_\ell$ and $q>q_u$ (see Fig. 2). However, for q in the interval $q_\ell < q < q_u$, there are three static states. The lower branch of this curve, with amplitudes in the range of $0 \le A \le A_u$ is called the unbuckled branch. The upper branch $(A \ge A_\ell)$ is called the buckled branch. The remaining states with amplitudes in the interval, $A_u \le A \le A_\ell$, lie on the intermediate branch.

As q increases from zero, the equilibrium states of the arch lie on the unbuckled branch. If q exceeds q_u, then the arch must jump dynamically toward the buckled state. Similarly, if the arch is in an equilibrium state corresponding to a point on the buckled state and q is slowly decreased below q, the arch will suddenly jump toward the unbuckled state. These dynamic transitions, which are called snap buckling, are obtained in Sec. IV by solving Eq. (6).

Consequently, the dimensionless pressures q_u and q_ℓ are called the upper and lower buckling loads, respectively. Their values are easily obtained from an elementary analysis of Eq. (8) as,

$$q_u = 4h\ell + 2D^{3/2}, \qquad q_\ell = 4h\ell - 2D^{3/2} \tag{10}$$

The corresponding values of the amplitudes are

$$A_u = h - D^{1/2}, \qquad A_\ell = h + D^{1/2} \tag{11}$$

The amplitude of the buckled state $A_b(q_u)$ corresponding to $q=q_u$ is obtained from Eq. (8) as

$$A_b(q_u) = 3h - 2A_u = h + 2D^{1/2} \tag{12}$$

It can be shown from an analysis of the linearized stability problem that the unbuckled and buckled branches are stable and the intermediate branch is unstable.

IV. The Dynamics of Snap Buckling

To analyze the snap buckling of the arch, we assume that $q=q_u$ and that the arch is in equilibrium at the limit point, $A=A_u$. A small initial displacement disturbance ϵ is given to the arch, so that,

$$A(0)=A_u+\epsilon, \qquad A'(0)=0 \tag{13}$$

The ensuing large-amplitude periodic motion describes the snap buckling of the arch. In our analysis, we assume that $\epsilon<0$. A similar analysis applies for $\epsilon>0$.

Since Eq. (6) represents a conservative mechanical system it has a first integral. By integrating this first integral we obtain a representation of the solution in terms of a Jacobian elliptic function and the roots of a quartic equation (see Ref. 6 for details). For small ϵ the roots are obtained by a perturbation method. This leads to a representation of the solution as a rational function of ϵ. The period T_0 in seconds of this periodic solution is given by

$$T_0=\frac{4\sqrt{2}K_0L}{\pi^2 3^{1/4}D^{1/4}}\left(\frac{\rho}{E}\right)^{1/2}(-\epsilon)^{-1/2}+0(1)$$

$$\approx\frac{1.206L}{D^{1/4}}\left(\frac{\rho}{E}\right)^{1/2}(-\epsilon)^{-1/2}+0(1) \tag{14}$$

where $K_0\equiv K[(2+\sqrt{3})/4]\approx 2.7693$ and $K(k)$ is the complete elliptic integral of the first kind with modulus k. In addition, the maximum amplitude W_m at the center of the arch during the motion is evaluated from Eq. (4) and the solution of Eq. (6) as

$$W_m=L[(H/L)+3D^{1/2}+0(\epsilon^3)] \tag{15}$$

V. Application to Drag-Reducing Compliant Walls

It is now shown that there are ranges of the geometrical parameters of the arch for which the amplitudes and frequency of the motion may be sufficiently large to produce drag reduction in accordance with Bushnell's conjecture.[3,4] The lateral force $P(X)$ and hence the parameter q is assumed to result from the mean pressure in the turbulent boundary layer acting on the top surface of the arch, and from an externally applied "vacuum" pressure p_0 acting on the under surface of the arch. In the analysis in Sec. IV and Ref. 6 it was assumed that p_0 was adjusted so that the resulting $q=q_u$. Then the disturbance ϵ triggered the periodic motion of the arch.

For an arch of rectangular cross section of breadth b and depth d, the parameters ℓ and D that are defined in Eqs. (2) and (9), respectively, are given by

$$\ell=(1/12)(d/L)^2, \quad D=\tfrac{1}{3}[(H/L)^2-(1/3)(d/L)^2] \tag{16}$$

Here $H=W^*(L/2)$ is the arch rise, i.e., it is the physical height of the center of the undeformed arch above the horizontal, see Eq. (3).

Typical dimensions (in inches) of panels used in drag reduction experiments[4-6] are

$$0.02\le L\le 0.035,\ 0.002\le H\le 0.003,\ 0.0001\le d\le 0.01 \tag{17a}$$

Then the parameters (H/L), (d/L), and D lie in the intervals,

$$0.07\le H/L\le 0.15,\ 0.005\le d/L\le 0.286,\ 0<D\le 0.0075 \tag{17b}$$

For (H/L) large compared to (d/L), then D, T_0, and W_m are given approximately by

$$D\approx\tfrac{1}{3}(H/L)^2,\ T_0\approx\frac{1.578L\sqrt{\rho/E}}{\sqrt{H/L}\sqrt{-\epsilon}},\ W_m\approx(1+\sqrt{3})H \tag{18}$$

If we denote the height of the arch at maximum displacement by H_m, then we obtain from Eq. (15)

$$H_m\equiv H+W_m=2H+3LD^{1/2}+0(\epsilon) \tag{19}$$

By substituting the maximum values of H, L, and D given in Eq. (17) into Eq. (19), we obtain for the maximum value of H_m

$$H_m\approx 0.015 \text{ in.} \tag{20}$$

Significantly smaller values of H_m are obtained for other values of H, L, and D in the ranges given in Eq. (17). For example, if H/L is large compared to d/L then using Eq. (18) in Eq. (19) we obtain

$$H_m\approx(2+\sqrt{3})H \tag{21}$$

Then by using the minimum value of H from Eq. (17a), we get $H_m\approx 0.0075$ in. In experiments conducted at NASA Langley[3,4] with other compliant wall structures, it was difficult to excite motions with amplitudes as small as 0.0008 in. *The present analysis suggests that amplitudes 10-20 times larger can be obtained using the snap buckling of curved structures.*

If the maximum amplitudes of compliant walls are too large, they will induce drag because of a "roughness" effect. For turbulent boundary-layer flows, an empirical rule for a hydraulically smooth surface is that the maximum amplitudes should not exceed 100 ν/U_∞, where ν is the kinematic viscosity of the fluid and U_∞ the freestream velocity of the flow.[9] For the typical experimental values of $\nu=1.5\times10^{-4}$ ft^2/s and U_∞ in the range of $3\le U_\infty\le 25$ ft/s, the empirical rule requires that the maximum amplitudes lie between 0.0072 and 0.06 in. The geometrical parameters H, L, and D can be selected so that the maximum amplitudes lie within these values.

Furthermore, it has been conjectured[3,4] from experiments and a study of data that wall frequencies $T_0^{-1}\approx 2000$ Hz are necessary for drag reduction. For this frequency, we conclude from Eq. (14) that the corresponding amplitude ϵ of the disturbance is given approximately by

$$-\epsilon\approx 582\times10^4(\rho/E)L^2/D^{1/2} \tag{22}$$

In Table 1, we give the values of $-\epsilon$ obtained from Eq. (22) for typical materials used in drag reduction studies. The values of ρ/E were obtained from Ref. 5.

To interpret the results in Table 1, we recall that ϵ represents a small displacement disturbance applied to the

Table 1 Disturbance amplitudes for 2000 Hz motions

Material	$\rho/E\times10^{10}$	$L^2/D^{1/2}=0.0046$	$-\epsilon\times10^5$ in. $=0.01$	$=0.05$	$=0.1$
Mylar	1.69	0.45	0.98	4.9	9.8
100 PPI foam[a]	3,600	959	2,088	10,440	20,880
RTV[b]	14,400	3,834	8,350	41,750	83,500

[a] 100 PPI foam is a polyurethane foam. [b] RTV is a silicon rubber.

arch. We observe from the table that at a frequency of 2000 Hz, Mylar would be a suitable material for a wide range of the geometric parameter $L^2/D^{1/2}$. That is, small disturbances can produce a periodic motion at the required frequency. The materials 100 PPI foam and RTV are suitable provided that $L^2/D^{1/2}$ is sufficiently small. Other materials such as polyvinylchloride (PVC) that have been used in drag reduction experiments are unsuitable because they require a relatively large value of $-\epsilon$ to excite the periodic motion with the required frequency.

The parameter ϵ crudely represents disturbances produced by airflow over the arch, such as turbulent boundary-layer fluctuations. If the magnitude of these fluctuations is known or can be measured in an experiment, then by using the analysis and results of the present investigation, it is possible to estimate the geometric and material properties of the arch that are necessary to produce the desired frequency and amplitude of response. These results apply only to initial disturbances of the form given in Eq. (3). If more complicated disturbances occur, then the response will contain more than one mode. Additional modes introduce more equilibrium states of the arch than are illustrated in Fig. 2, see, e.g., Ref. 8.

Aerodynamic and structural damping have been neglected in the present analysis. If there is a small amount of structural damping, then instead of snap buckling occurring as a periodic oscillation, there will be a damped oscillation with the solution approaching the buckled equilibrium state as $t \to \infty$. That is, energy is lost by the system due to damping, and the arch eventually comes to rest at the buckled equilibrium point. In order to maintain a periodic oscillation, energy must be supplied to the arch from its environment to replace the energy lost by dissipation. This energy may be obtained from the pressure induced by aerodynamic forces and from turbulent boundary-layer fluctuations. For example, the turbulent boundary-layer fluctuations may provide sufficient disturbances to the arch at regular intervals to continually excite a periodic, or nearly periodic, large-amplitude oscillation. However, the aerodynamic forces may also damp the motion. A more sophisticated study is required to determine whether the net energies supplied to the arch by the aerodynamic pressures and turbulent boundary fluctuations are sufficient. Then it is necessary to consider the coupled aerodynamic/structural interaction problem.

Acknowledgments

The research reported in this paper was supported at the Applied Institute of Mathematics, Inc. by the Fluid Mechanics Branch, NASA Langley Research Center under Contract NAS1-14717. The author wishes to thank Dr. Dennis Bushnell for introducing him to the subject and for many stimulating conversations.

References

[1] Kramer, M. O., "Hydrodynamics of the Dolphin," *Advances in Hydroscience*, Vol. 2, Academic Press, New York, 1965, p. 111.

[2] Kramer, M. O., "The Drag Reduction of Fast Underwater Bodies with the Aid of an Artificial Dolphin Skin," *Jahrbuch der Deutschen Gesellshaft fur Luft- und Raumfahrt*, Blenk and Schutz, Cologne, 1969, p. 102.

[3] Bushnell, D. M., Hefner, J. N., and Ash, R. L., "Effect of Compliant Wall Motion on Turbulent Boundary Layers," *Physics of Fluids*, Vol. 20, 1977, pp. 531-548.

[4] Ash, R. L., Bushnell, D. M., Weinstein, L. M., and Balasubramanian, R., "Compliant Wall Surface Motion and Its Effect on the Structure of a Turbulent Boundary Layer," Paper presented at Fourth Biennial Symposium on Turbulence in Liquids, University of Missouri, Rolla, 1975.

[5] Fischer, M. C., Weinstein, L. M., Ash, R. L., and Bushnell, D. M., "Compliant Wall-Turbulent Skin-Friction Reduction Research," AIAA Paper 75-833, 1975.

[6] Reiss, E. L., "A New Asymptotic Method for Jump Phenomena," *SIAM Journal on Applied Mathematics*, Vol. 39, 1980, pp. 440-455.

[7] Hoff, N. J. and Bruce, V. G., "Dynamic Analysis of the Buckling of Laterally Loaded Flat Arches," *Journal of Mathematics and Physics (Cambridge, Mass.)*, Vol. 32, 1954, pp. 276-288.

[8] Kaplan, A. and Fung, Y. C., "Buckling of Low Arches or Curved Beams of Small Curvature," NACA TN 2840, 1952.

[9] Schlichting, H., *Boundary-Layer Theory*, 6th Ed., McGraw-Hill Book Co., New York, 1968.